

Synthesis of $\text{Ti}(\text{OH})\text{OF} \cdot 0.66 \text{H}_2\text{O}$ in Imidazolium-based Ionic Liquids

Melanie Sieland,^[a] Valentine Camus-Genot,^[a, b] Igor Djerdj,^[c] and Bernd M. Smarsly^{*[a, d]}

The influence of the cation of imidazolium-derived ionic liquids (ILs) on a low-temperature solution-based synthesis of hexagonal tungsten bronze (HTB) type $\text{Ti}(\text{OH})\text{OF} \cdot 0.66 \text{H}_2\text{O}$ and bronze-type $\text{TiO}_2(\text{B})$ is investigated. The IL ($\text{C}_x\text{mim BF}_4$) acts as solvent and also as reaction partner with respect to the decomposition of $[\text{BF}_4]^-$, releasing F^- . In the present study, the chain length of the alkyl chain side groups attached to the imidazolium ring was varied ($\text{C}_2\text{mim BF}_4$ to $\text{C}_{10}\text{mim BF}_4$), and the obtained solids were analyzed by Powder X-Ray diffraction (PXRD) followed by Rietveld refinement. As a main finding these analyses indicate a transformation of $\text{Ti}(\text{OH})\text{OF} \cdot 0.66 \text{H}_2\text{O}$ into $\text{TiO}_2(\text{B})$, and upon

prolonged reaction time finally also into anatase TiO_2 . Rietveld analysis suggests that when using ILs with longer alkyl chains, the conversion of $\text{Ti}(\text{OH})\text{OF} \cdot 0.66 \text{H}_2\text{O}$ is slower compared to syntheses performed with smaller alkyl chains. Hence, $\text{Ti}(\text{OH})\text{OF} \cdot 0.66 \text{H}_2\text{O}$ appears to be metastable and is stabilized by long-chain ILs serving as surfactant attached to the crystallites' surface. In this view, the ILs shield the nanoparticles and thus slow down the conversion into the more stable compounds. This confirms previous findings that ILs act as both, solvent and reaction medium in this reaction, thus enabling the synthesis of peculiar Ti-oxides.

1. Introduction

Syntheses of metal oxides in ionic liquids (ILs) have gained a lot of interest in recent years. Various studies have shown that it is possible to prepare different metal oxides with the help of ILs, for example RuO_2 , ZnO and MoO_3 .^[1] The advantages of syntheses utilizing ILs are often a smaller number of reaction steps and a low reaction temperature.^[2] Many of these syntheses are therefore in agreement with the concept of

“green chemistry” which makes the use of ILs as reaction medium a promising strategy for future materials synthesis.^[3]

TiO_2 has meanwhile been produced in different modifications and morphologies with the help of ILs as solvent and reaction partner.^[4] Various working groups have succeeded in synthesizing anatase in ionic liquids at quite low temperatures, compared to other types of sol-gel syntheses. Different morphologies were obtained, for example microspheres, nanoparticles, mesoporous particles or nanoparticles.^[5] Besides anatase, it is also possible to synthesize rutile with varying morphologies, like nanoparticles and nanoflowers, by means of ILs.^[6]

In contrast to these well-known titania modifications, it is also possible to synthesize less known titania and Ti-oxo compounds with the help of ILs, for example the bronze-phase modification $\text{TiO}_2(\text{B})$.^[7] This compound is a metastable modification of TiO_2 and possesses a sheet-like crystal structure (see Figure 1b)) which is the reason why this compound exhibits the second lowest density of all known titania modifications.^[8] In classic syntheses of this compound usually quite harsh conditions such as calcination steps at 1000°C for several days were needed.^[8,9] In contrast, Wessel et al. presented an IL-based synthesis route for phase-pure $\text{TiO}_2(\text{B})$ under quite soft conditions.^[10] In this synthesis, imidazolium-based ILs were used, and 95°C were sufficient as reaction temperature, providing nanocrystalline $\text{TiO}_2(\text{B})$. Voepel et al. further developed the synthesis procedure and studied the formation mechanism by in-situ studies.^[11] Additionally, it was found that the concentration of the IL-anion $[\text{BF}_4]^-$ markedly influences the composition of the obtained products. During the reaction the IL-anion $[\text{BF}_4]^-$ is slowly hydrolyzed to $[\text{B}(\text{OH})_4]^-$, i.e. releasing fluoride anions, which coordinate to Ti chloro complexes in apical position of Ti^{4+} and therefore inhibit the hydrolysis at this position, thus pre-determining the sheet-like arrangement of TiO_6 -octahedra in $\text{TiO}_2(\text{B})$.^[11] Depending on the fluoride

[a] M. Sieland, V. Camus-Genot, Prof. B. M. Smarsly
Institute of Physical Chemistry
Justus Liebig University
Heinrich-Buff-Ring 17
35392 Giessen (Germany)
E-mail: Bernd.Smarsly@phys.chemie.uni-giessen.de

[b] V. Camus-Genot
Institut des Molécules et des Matériaux du Mans
UMR CNRS 6283
Le Mans Université
Avenue Olivier Messiaen
72085 Le Mans Cedex 9 (France)

[c] Prof. I. Djerdj
Department of Chemistry
Josip Juraj Strossmayer University of Osijek
Cara Hadrijana 8/A
31000 Osijek (Croatia)

[d] Prof. B. M. Smarsly
Center of Materials Research
Justus Liebig University
Heinrich-Buff-Ring 16
35392 Giessen (Germany)

Supporting information for this article is available on the WWW under <https://doi.org/10.1002/open.202000256>

An invited contribution to a Special Issue dedicated to Material Synthesis in Ionic Liquids

© 2020 The Authors. Published by Wiley-VCH GmbH. This is an open access article under the terms of the Creative Commons Attribution Non-Commercial NoDerivs License, which permits use and distribution in any medium, provided the original work is properly cited, the use is non-commercial and no modifications or adaptations are made.

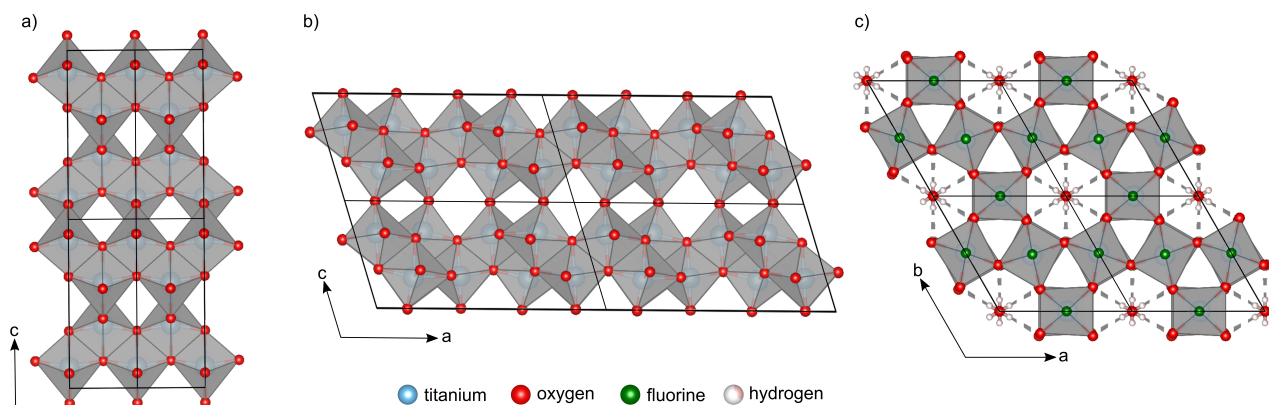
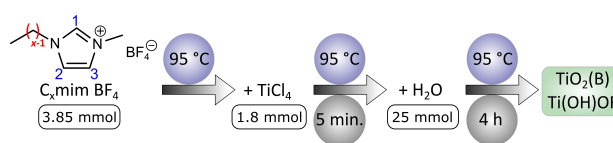


Figure 1. a) 2×2 supercell of anatase. b) 2×2 supercell of $\text{TiO}_2(\text{B})$. c) 2×2 supercell of $\text{Ti}(\text{OH})\text{OF} \cdot 0.66 \text{H}_2\text{O}$.

concentration, a different number of positions are blocked, leading to the formation of different Ti-oxyfluorides. With no $[\text{BF}_4]^-$ present, mainly rutile was observed as product. Upon increasing fluoride content Voepel et al. were able to synthesize anatase and $\text{TiO}_2(\text{B})$, and with a very high fluoride anion concentration it was even possible to synthesize the hexagonal tungsten bronze (HTB) compound $\text{Ti}(\text{OH})\text{OF} \cdot 0.66 \text{H}_2\text{O}$. This solid compound has a quite particular crystal structure featuring channels along the *c*-axis (see Figure 1c).^[12] It was shown that this material might possess quite interesting electrochemical properties which renders this compound a promising battery material.^[13] In conclusion, while the role of the IL-anion during the presented reaction has therefore been clarified relatively well, the role of the IL-cation during the reaction remains unclear: while the imidazolium ring and attached alkyl chains should be chemically stable under the reaction conditions, the amphiphilic character of these ILs can possibly affect the nucleation and crystallization.

The goal of this study is to investigate the influence of the cations in imidazolium-based ILs on the reaction, in particular the dimension of the alkyl chains attached to the imidazolium ring, which alters the amphiphilic nature of the IL. Our previous studies had suggested the formation of self-assembled entities such as micelles of the imidazolium-based ILs. It was discussed that these micelles might lead to a higher local $[\text{BF}_4]^-$ concentration and therefore promote the formation of $\text{TiO}_2(\text{B})$ or $\text{Ti}(\text{OH})\text{OF} \cdot 0.66 \text{H}_2\text{O}$. These previous results indeed showed that there is a certain impact of the IL alkyl chain length on the received products, as it was possible to synthesize different products varying the concentration of the IL cations used ($[\text{C}_4\text{mim}]^+$ and $[\text{C}_{16}\text{mim}]^+$), but so far no systematic study has been performed addressing the role of the alkyl chain. Hence, in the present study we use the reproducible and well established synthesis of $\text{Ti}(\text{OH})\text{OF} \cdot 0.66 \text{H}_2\text{O}$ and $\text{TiO}_2(\text{B})$ already described in earlier works of our working group (see Scheme 1) to study the influence of the IL cation on the reaction, by variation of the alkyl chain length, from $\text{C}_2\text{mim BF}_4$ to $\text{C}_{10}\text{mim BF}_4$, thereby increasing the amphiphilic character.^[11,13] The obtained solids were subjected to in-depth XRD analysis



Scheme 1. Schematic illustration of the used synthesis procedure. In this work *x* was varied from 2 to 10.

using Rietveld refinement, and by determining the overall mass of the products it was possible to quantify the composition of the mixtures.

2. Results and Discussion

In order to understand the role of the cation in the reaction mechanism we focused on the influence of the length of the alkyl chain of the used imidazolium-based ILs on the reaction products, which were investigated by X-ray diffraction (XRD), providing a quantitative phase analysis by means of Rietveld refinement. For the XRD measurements $\text{CuK}\alpha_1$ ($\lambda = 1.540560 \text{ \AA}$) radiation was used. In addition, the mass of the received products was determined in order to obtain information about the reaction mechanism, by calculating the absolute amounts of the different products, using the relative fractions obtained from Rietveld analysis.

Thus, syntheses applying different ILs ranging from $\text{C}_2\text{mim BF}_4$ to $\text{C}_{10}\text{mim BF}_4$ were performed, while all other synthesis parameters were kept identical. It is important to notice that the amount (3.85 mmol) and not the total mass of ILs was kept constant in this study. The synthesis typically provides $\text{Ti}(\text{OH})\text{OF} \cdot 0.66 \text{H}_2\text{O}$ and small amounts of $\text{TiO}_2(\text{B})$ after a reaction time of 4 h using $\text{C}_4\text{mim BF}_4$.

The obtained X-Ray diffractograms show gradual differences to each other while the XRD pattern of the sample with $x=2$ differs significantly from the XRD patterns of the other samples (Figure 2). Upon the synthesis performed with $\text{C}_2\text{mim BF}_4$ the reflections are quite broad, speaking for ill-defined crystallinity. Also, a large fraction of $\text{TiO}_2(\text{B})$ is obtained next to $\text{Ti}(\text{OH})$

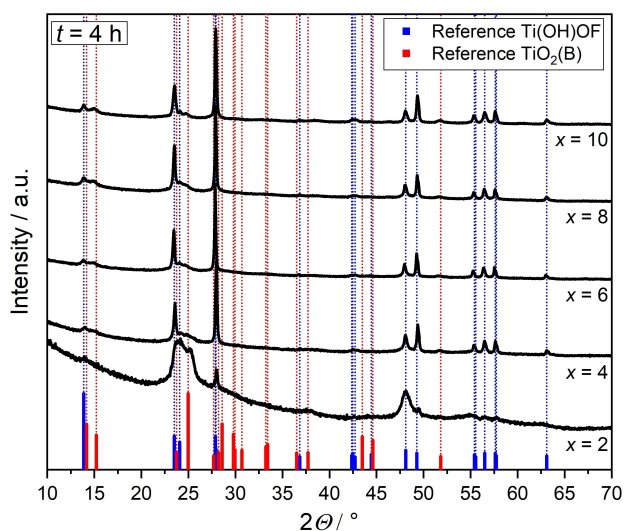


Figure 2. PXRD patterns and reference patterns (solid bars) of the products received after syntheses with different ILs ($C_x\text{mim BF}_4$) after 4 h. The blue bars represent the reference pattern of $\text{Ti(OH)OF} \cdot 0.66 \text{H}_2\text{O}$ (based on ref. 12) and the red bars represent the reference pattern of $\text{TiO}_2(\text{B})$ (based on ref. 8).

$\text{OF} \cdot 0.66 \text{H}_2\text{O}$. In contrast, the synthesis based on $C_{10}\text{mim BF}_4$ resulted in a more defined XRD pattern, and the product is composed primarily of the targeted $\text{Ti(OH)OF} \cdot 0.66 \text{H}_2\text{O}$.

As a first result, these differences qualitatively show that the dimension of the used IL-cation does influence the reaction pathway and the received products. To understand the impact in further detail, ex-situ XRD studies were carried out as a function of the reaction time. Figure 3 shows an ex-situ XRD study of a synthesis performed with $C_4\text{mim BF}_4$. It can be clearly seen that in all diffractograms $\text{Ti(OH)OF} \cdot 0.66 \text{H}_2\text{O}$ is present. Beside $\text{Ti(OH)OF} \cdot 0.66 \text{H}_2\text{O}$, $\text{TiO}_2(\text{B})$ is also observed in all cases, which can be recognized by the pronounced reflection at $2\theta = 15.2^\circ$. It is also noticeable that after 10 h additional reflections can be observed for the first time, which can be assigned to the anatase phase. This change in the XRD pattern suggests that after a longer reaction time a conversion of the obtained products to anatase might occur.

In order to obtain quantitative information on the phase composition of the different reaction products and thus to address the possible transformation of the different Ti-oxides, Rietveld refinement analyses were carried out. The relative phase compositions obtained by this method are shown in Figure 4a), and additional information about the refinements can be found in the Supporting Information file. Figure 4a) presents the relative amounts of the different products calculated by Rietveld refinement from the respective XRD data. The relative amount of $\text{Ti(OH)OF} \cdot 0.66 \text{H}_2\text{O}$ decreases with time while the relative amount of $\text{TiO}_2(\text{B})$ increases. In addition, after 10 h anatase is present for the first time (see Figure 3).

As the overall mass of the solid products was determined in each case, the relative amounts evaluated by Rietveld refinements were converted into absolute amounts of the single compounds (Figure 4b). It can be clearly seen that the absolute amount of $\text{Ti(OH)OF} \cdot 0.66 \text{H}_2\text{O}$ initially increases, because of

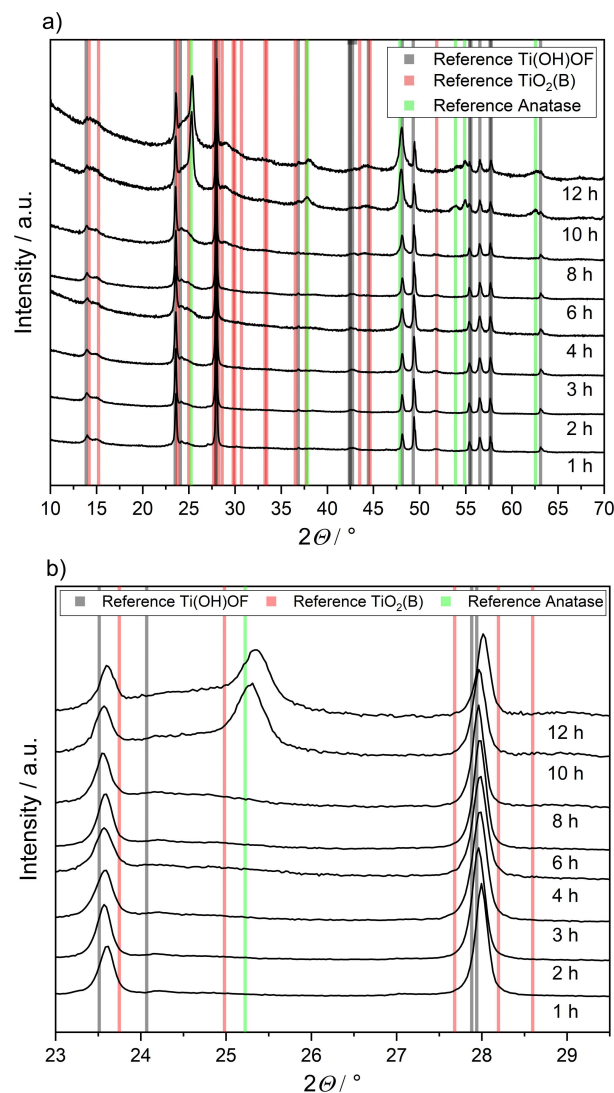


Figure 3. Ex-situ XRD-study of syntheses performed with $C_4\text{mim BF}_4$. a) shows the full measured pattern, b) shows a different magnification of the patterns, another magnification can be found in the Supporting Information file (see Figure S1). The reference bars of $\text{Ti(OH)OF} \cdot 0.66 \text{H}_2\text{O}$ are based on ref. 12, the reference bars of $\text{TiO}_2(\text{B})$ are based on ref. 8, and the reference bars of anatase are based on ref. 20.

nucleation from solution. Surprisingly, after 4 h reaction time the absolute amount of this compound significantly decreases. At the same time the amount of $\text{TiO}_2(\text{B})$ increases continuously, which proves that a conversion of $\text{Ti(OH)OF} \cdot 0.66 \text{H}_2\text{O}$ to $\text{TiO}_2(\text{B})$ takes place during the reaction.

In principle there are two different transformation pathways that can take place at this point (see Scheme 2). On the one hand, a direct solid-to-solid conversion of $\text{Ti(OH)OF} \cdot 0.66 \text{H}_2\text{O}$ to $\text{TiO}_2(\text{B})$ might occur. The other possible mechanism could be a dissolution of $\text{Ti(OH)OF} \cdot 0.66 \text{H}_2\text{O}$ followed by a rapid nucleation and crystallization of $\text{TiO}_2(\text{B})$. Which of the two processes actually takes place can in principle be assessed by calculating the absolute amount of $\text{Ti(OH)OF} \cdot 0.66 \text{H}_2\text{O}$ which disappears and the absolute amount of formed $\text{TiO}_2(\text{B})$. If these two values coincided for all times, a solid-to-solid transition would be

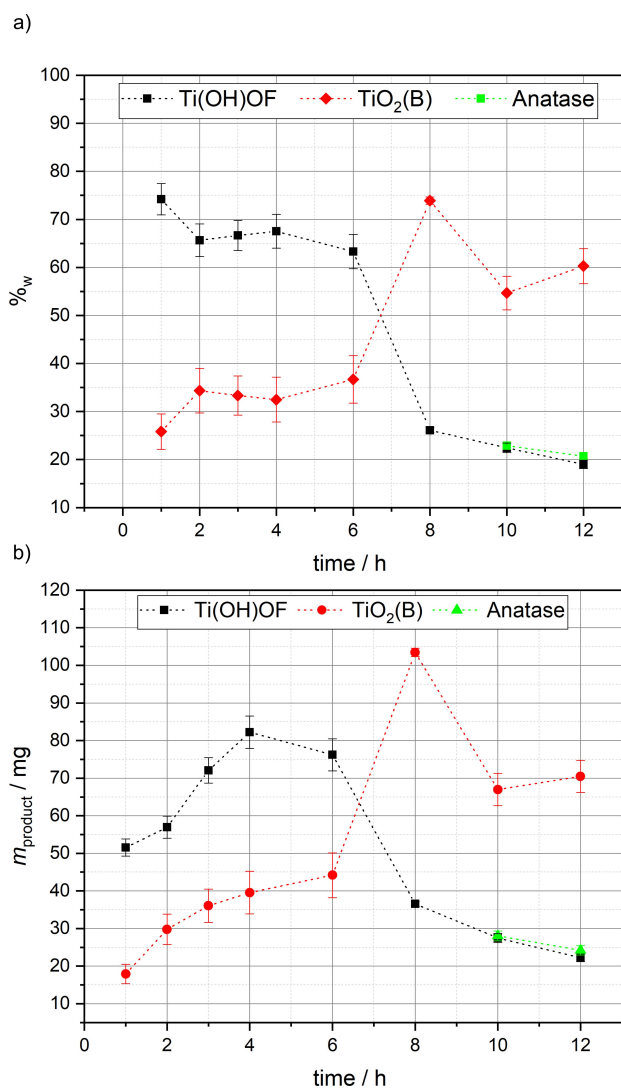
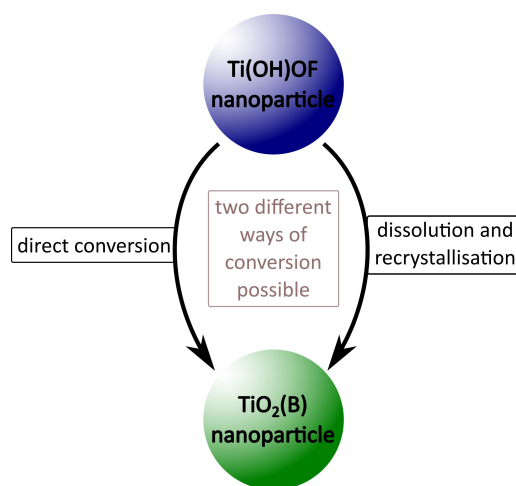


Figure 4. a) Relative phase composition of the different products of the ex-situ time study with $C_4\text{mim BF}_4$. The results were obtained by Rietveld refinements. b) Absolute amounts of the different phases inside of the products. The results were calculated with the help of the relative amounts and the measured mass of the products.

probable. It is seen that these two values show marked variation as a function of time, varying between 1 and 2.09 for different times, so that a clear differentiation between these two pathways (Scheme 2) is not possible. Yet, the ratio of the amount of formed $\text{TiO}_2(\text{B})$ to the amount of disappeared $\text{Ti(OH)OF} \cdot 0.66 \text{H}_2\text{O}$ is always larger than “one”, implying that at a portion of the formed $\text{TiO}_2(\text{B})$ is not generated from $\text{Ti(OH)OF} \cdot 0.66 \text{H}_2\text{O}$, but, for example, by nucleation from solution.

The conversion of $\text{Ti(OH)OF} \cdot 0.66 \text{H}_2\text{O}$ to $\text{TiO}_2(\text{B})$, which is present in this reaction, indicates that $\text{TiO}_2(\text{B})$ is thermodynamically more stable than $\text{Ti(OH)OF} \cdot 0.66 \text{H}_2\text{O}$ under the present conditions. Interestingly, after 10 hours a further conversion of the products to anatase can be observed. Since anatase is, beside rutile, one of the most thermodynamically stable TiO_2 modifications, it is reasonable that at a certain point in the



Scheme 2. Illustration of the two possible conversion mechanisms that could take place during the reaction.

synthesis the resulting products are converted into this compound, nicely following Ostwald’s step rule.

In addition to the phase composition, the results of the Rietveld refinements show that the average apparent crystallite size of the products does not change significantly over time (see Figure S4 in Supporting Information). This finding also speaks for a direct solid-solid transition, as a dissolution process should be accompanied by a decrease in crystallite dimension.

In order to evaluate the influence of the alkyl chain length on the synthesis, a similar time-dependent study was performed using $C_{10}\text{mim BF}_4$, containing a significantly longer alkyl chain. Figure 5 shows the XRD patterns of the products as a function of the reaction time.

It can be observed that in all samples a large amount of $\text{Ti(OH)OF} \cdot 0.66 \text{H}_2\text{O}$ and a rather small amount of $\text{TiO}_2(\text{B})$ is present. After 12 h hours, reflections of the anatase phase appeared for the first time, that is, later than compared to the corresponding study using $C_4\text{mim BF}_4$ (see Figure 3).

In order to obtain quantitative results on the phase composition of the mixtures, Rietveld refinement analyses were carried out. The relative and absolute phase compositions of the syntheses with $C_{10}\text{mim BF}_4$ in comparison to syntheses performed with $C_4\text{mim BF}_4$ are summarized in Figure 6.

Figure 6a) shows the relative amount of $\text{Ti(OH)OF} \cdot 0.66 \text{H}_2\text{O}$ obtained in the syntheses directly comparing $C_4\text{mim BF}_4$ and $C_{10}\text{mim BF}_4$. It is noticeable that regardless of the size of the alkyl chains, the same trends can be observed in both reactions, that means for both chain lengths the relative amount of $\text{Ti(OH)OF} \cdot 0.66 \text{H}_2\text{O}$ decreases. It is noticeable, however, that in the reaction involving $C_{10}\text{mim BF}_4$ the relative amount of $\text{Ti(OH)OF} \cdot 0.66 \text{H}_2\text{O}$ seems to decrease by a slower rate. The fraction of $\text{TiO}_2(\text{B})$ increased with reaction time for both ILs. Yet, there are systematic differences between the two syntheses, since the relative amount of $\text{TiO}_2(\text{B})$ increases more strongly in the

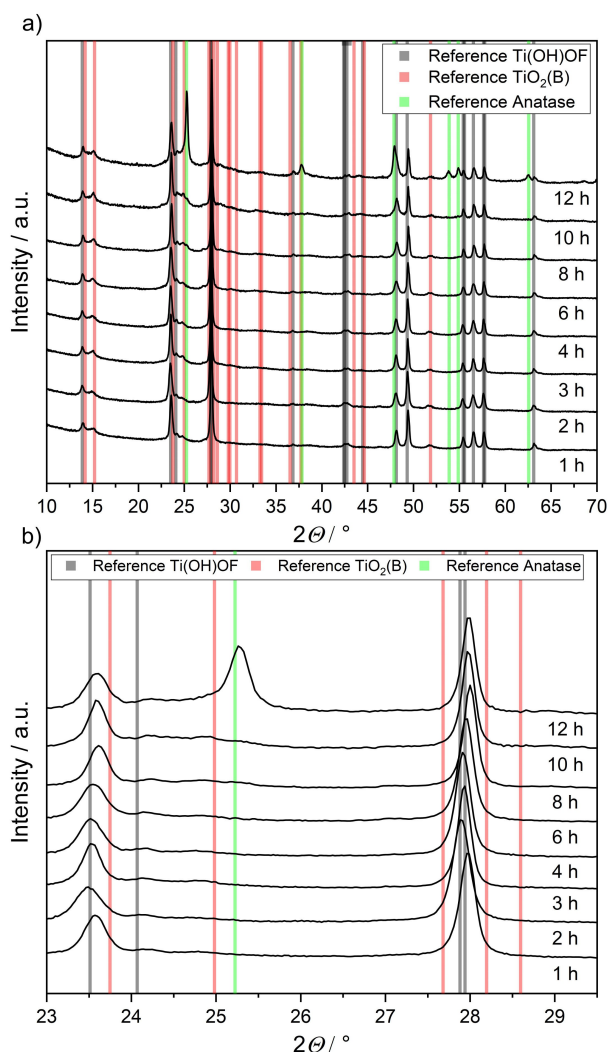
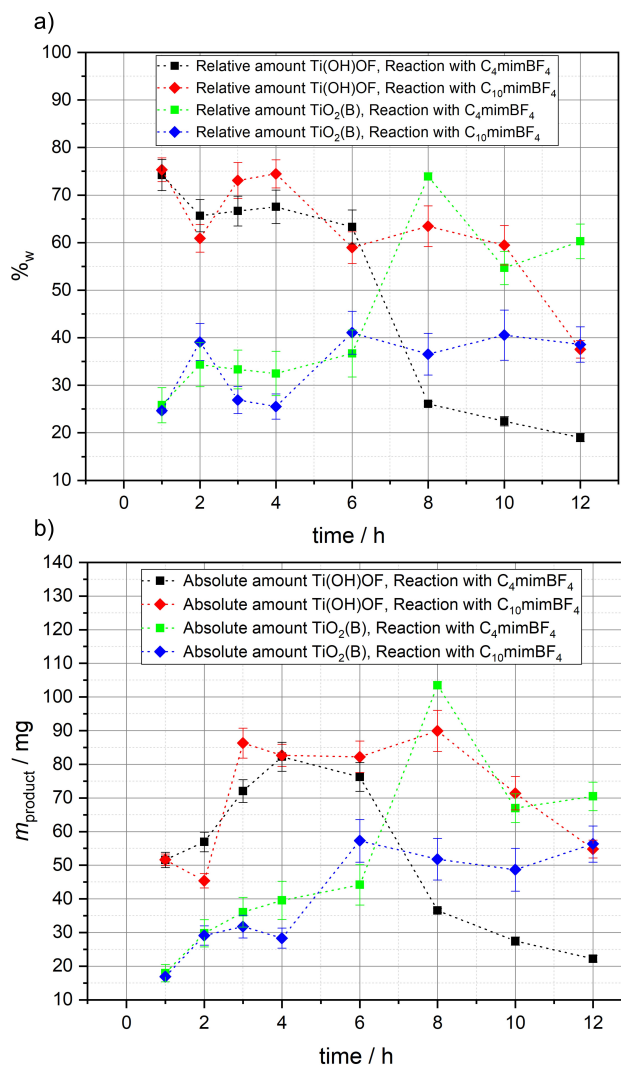


Figure 5. Ex-situ XRD-study of syntheses performed with C₁₀mim BF₄. a) shows the full measured pattern, b) shows a different magnification of the patterns, another magnification can be found in the Supporting Information file (see Figure S2). The reference bars of Ti(OH)OF·0.66 H₂O are based on ref. 12, the reference bars of TiO₂(B) are based on ref. 8, and the reference bars of anatase are based on ref. 20.

synthesis with C₄mim BF₄ than in the synthesis with C₁₀mim BF₄.

Figure 6b) shows the progress of the absolute amount of Ti(OH)OF·0.66 H₂O and TiO₂(B) for these two ILs. For Ti(OH)OF·0.66 H₂O the absolute amount first increases in both syntheses, and starts to decrease after a certain period of time. It is noticeable that in the reaction with C₄mim BF₄ this decrease occurs after 4 h, whereas in the reaction with C₁₀mim BF₄ a decrease can be observed at a substantially later time, namely after 8 h. In addition, the absolute and relative amount of Ti(OH)OF·0.66 H₂O tends to be higher for the reaction with C₁₀mim BF₄. By contrast, the amount of TiO₂(B) increases constantly, while the absolute and relative amount are higher in syntheses using C₄mim BF₄.



c)

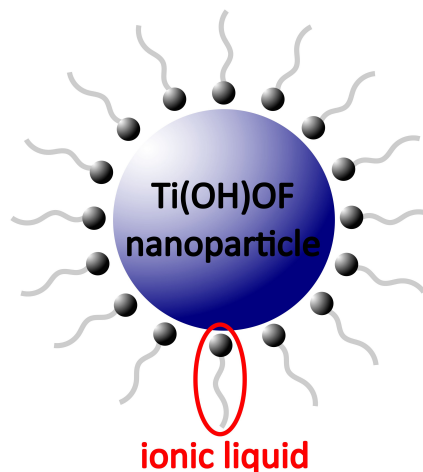


Figure 6. a) Relative amount of Ti(OH)OF·0.66 H₂O and TiO₂(B) obtained in the different syntheses. b) Absolute amounts of Ti(OH)OF·0.66 H₂O and TiO₂(B) obtained in the different syntheses. c) Schematic illustration of the stabilization of the built nanoparticles.

These observations show that by using an IL with a longer alkyl chain the conversion of Ti(OH)OF·0.66 H₂O is impeded. As

a result, the conversion of this compound into $\text{TiO}_2(\text{B})$ is slower, when using $\text{C}_{10}\text{mim BF}_4$, and less $\text{TiO}_2(\text{B})$ is present in this synthesis at the same time in comparison to $\text{C}_4\text{mim BF}_4$.

One explanation for the observed trends could be that larger alkyl chains of the ILs are able to stabilize the formed nanoparticles against transformation, by acting as a surfactant attached to the particles' surface (Figure 6c). An interaction and a resulting stabilization of built nanoparticles by imidazolium-based ILs was already shown in other studies. Zheng et al.^[14] have shown that the ionic liquid Emim Br is able to influence the crystal structure and morphology of rutile, which is a result of two different interactions. Firstly, the H1-atom (see Scheme 1) of the imidazolium ring carries a partial positive charge, due to the delocalization of the positive charge within the imidazolium ring, and is therefore able to form hydrogen bonds with the O atoms of TiO_2 . Studies have shown that such an interaction is possible in an environment with $\text{pH} < 3.5$.^[15] The interaction results in a coordination of the imidazolium ring on the surface of the nanoparticle and an arrangement of the alkyl-chains of the IL around the particle (Figure 6c). Secondly, this study found π - π stacking interactions between the cations, which can form a coverage layer on the surface of the nanoparticle. Such layer of IL cations on the surface of a particle inhibits the transport of atoms or small molecules from or to the surface and can therefore stabilize the product against dissolution and solid-solid transformation.

Ott et al.^[16] studied the stabilization of transition-metal nanoclusters by imidazolium-based ILs as well. They showed that the positive charge of the imidazolium ring leads to a N-heterocyclic carbene formation at the metal surface which is able to stabilize transition-metal nanoclusters.

In our reaction we use imidazolium-based ILs, and TiCl_4 causing a low pH-value in the reaction solution. Therefore, an interaction between the H1 atom and the surface of the nanoparticle is plausible as well. The observed stabilization of the built products by ILs with longer alkyl-chains could be explained by the π - π stacking interactions between the cations. The resulting coverage layer of the surface is larger when using $\text{C}_{10}\text{mim BF}_4$ in comparison to using $\text{C}_2\text{mim BF}_4$. This layer slows down the conversion by impeding transport of small molecules (Ti-complexes, fluoride ions, etc) from or to the particles' surface. Also, attached IL can aggravate the rearrangement of the interior crystallite structure. Thus, the larger the constituents of an ionic liquid, the more pronounced is the shielding and stabilization, and therefore the overall conversion would be slower. This qualitatively explains the observed differences in the synthesis with the long-chain IL $\text{C}_{10}\text{mim BF}_4$.

The hypothesis can be further supported by looking at the ex-situ time study using an IL with a quite short alkyl chain, that is, $\text{C}_2\text{mim BF}_4$. In this case (Figure 7) broad XRD reflections are obtained, speaking for defect-rich and small nanocrystals. This result further confirms that the IL-cation substantially influences the crystallization of the Ti-oxides. In addition, it can be observed that anatase, which is the thermodynamically most stable of the involved compounds,

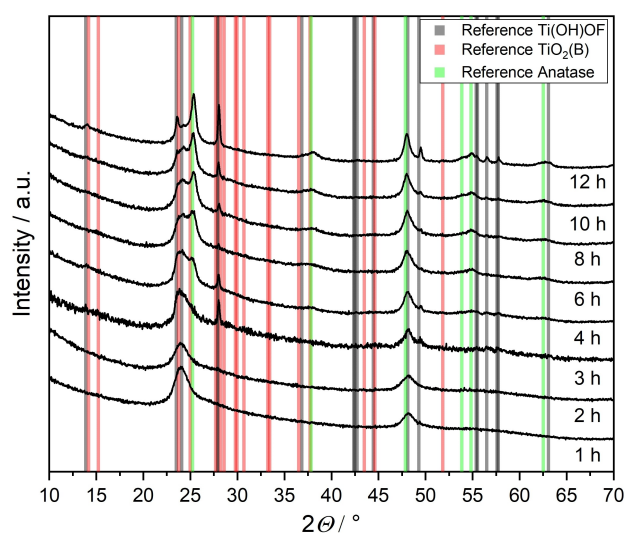


Figure 7. Ex-situ XRD-study of syntheses performed with $\text{C}_2\text{mim BF}_4$, other magnifications of the patterns can be found in the Supporting Information file (see Figure S3) The reference bars of $\text{Ti(OH)OF} \cdot 0.66 \text{H}_2\text{O}$ are based on ref. 12, the reference bars of $\text{TiO}_2(\text{B})$ are based on ref. 8. and the reference bars of anatase are based on ref. 20.

is already present after a synthesis time of only 3 h, which is much faster than in the other two ex-situ studies. These observations are consistent with the assumption that ILs bind to the particles' surface, thereby impede crystal growth and the conversion into other Ti oxides, that is, they can stabilize the nanoparticles. In case of $\text{C}_2\text{mim BF}_4$, the surfactant-like action is moderate, implying weak stabilization against chemical transformation. Hence, a relatively fast transformation of $\text{Ti(OH)OF} \cdot 0.66 \text{H}_2\text{O}$ into anatase occurs. Rietveld refinement confirms that also in this case the average apparent crystallite size of the products does not change significantly over time (see Figure S5 in Supporting Information).

It should be noted that using an IL with a longer alkyl chain increases the viscosity of the reaction solution, which could in principle influence the crystallization of the different products. However, the obtained results show that in the ex-situ studies with $\text{C}_4\text{mim BF}_4$ and $\text{C}_{10}\text{mim BF}_4$ comparable masses of products were received (see Figure S6 in Supporting Information). In addition, the crystallite size of the products is comparable (see Figures S4 and S5). Therefore we believe that the viscosity of the reaction solution does not influence the crystallisation of the products significantly.

3. Conclusion

In this work we investigated the influence of variations in the IL-cation on a low-temperature synthesis of the crystalline solid $\text{Ti(OH)OF} \cdot 0.66 \text{H}_2\text{O}$. For this purpose, we performed several studies varying the reaction times, applying imidazolium-based ILs with different lengths of the alkyl

chain attached to the positively charge imidazolium ring, ranging from $C_2\text{mim BF}_4$ to $C_{10}\text{mim BF}_4$.

The phase compositions of the products were determined from XRD by means of Rietveld refinement, and also the absolute mass of the product was determined. It is found that the absolute amount of $\text{Ti}(\text{OH})\text{OF} \cdot 0.66 \text{H}_2\text{O}$ first increases and then decreases over time while the amount of the Bronze-type $\text{TiO}_2(\text{B})$ constantly increases, suggesting that a conversion of $\text{Ti}(\text{OH})\text{OF} \cdot 0.66 \text{H}_2\text{O}$ into $\text{TiO}_2(\text{B})$ occurs. The detailed mechanism of such interesting transformation can be further investigated, for example with the help of theoretical approaches similar to recent studies by Macchieraldo et al.^[21]

In addition, a comparison of the different reaction-time-dependent studies implies that the used imidazolium-based ionic liquids are probably capable of attaching their polar imidazolium head group to the particles' surface, thereby stabilizing the formed $\text{Ti}(\text{OH})\text{OF} \cdot 0.66 \text{H}_2\text{O}$ nanoparticles. This stabilization inhibits the conversion of the nanoparticles into $\text{TiO}_2(\text{B})$ when using long-chain ILs in comparison to reactions involving ILs with smaller alkyl chains, and thus slows down the process. To validate these results further studies should be carried out focusing on a constant absolute mass of the ILs used instead of using a constant amount. Also other analytical methods, for example, Raman spectroscopy, can assist in the determination of the relative amounts of the intermediates, in combination with supporting theoretical approaches.^[21]

It was not yet possible to synthesize phase-pure $\text{Ti}(\text{OH})\text{OF} \cdot 0.66 \text{H}_2\text{O}$ with the presented synthesis. The results of this work show that a conversion of $\text{Ti}(\text{OH})\text{OF} \cdot 0.66 \text{H}_2\text{O}$ to $\text{TiO}_2(\text{B})$ takes place. It should therefore be possible to synthesize phase-pure $\text{Ti}(\text{OH})\text{OF} \cdot 0.66 \text{H}_2\text{O}$ by adapting the synthesis conditions, preventing the transformation.

The results of this study show once again that ILs act as both, solvent and reaction medium in such solution-based reactions with high IL concentrations. In addition, they not only act as a solvent and donor of fluoride, but also influence the crystallization by their interaction with solids, probably similar to surfactants. In this respect, the present study adds a further factor in understanding the synthesis of solids in ILs.

Experimental Section

Synthesis procedure

All ILs used in this work were purchased from IoLiTec, TiCl_4 was purchased from Merck. All chemicals were used without further purification or modification.

In a typical synthesis (see Scheme 1) 3.85 mmol IL ($C_x\text{mim BF}_4$ with $x=2-10$) were heated up to 95°C in a 25 mL two-necked flask. In the next step 0.2 mL (1.82 mmol) TiCl_4 were added under stirring (approx. 290 rpm). After stirring the solution for 5 minutes, 0.45 mL H_2O (25 mmol) were added drop wise (caution: TiCl_4 heavily reacts with water under release of gaseous HCl). The solution obtained was then kept at 95°C for different

periods of time, ranging from 0.5 h up to 12 h. After the solution has cooled down the built nanoparticles were washed 4 times with technical ethanol and dried.

Characterization techniques

To determine the phase composition of the received products Powder X-Ray diffraction (PXRD) experiments were carried out. The experiments were conducted with an Xpert Pro diffractometer (PANalytical instruments). For the measurements the instrument was operated at 40 kV and 40 mA and $\text{CuK}\alpha_1$ ($\lambda = 1.540560 \text{ \AA}$) radiation was used.

The Rietveld refinements were performed with the software FULLPROF, using the modified Thompson-Cox-Hastings pseudo-Voigt function as the profile function.^[17] This function was chosen because it allows an easy separation of size and microstrain contributions to profile broadening.^[18] However, in this case, it was only possible to extract average crystallite sizes since Caglioti parameter U tends to be around zero, disabling microstrain calculation. The phase composition was calculated using the well-known procedure of Hill and Howard.^[19]

Acknowledgements

M.S. and B.M.S. kindly acknowledge the DFG for funding within the priority program SPP1708 and strong support of the Center of Materials Research (ZfM/LaMa, Giessen) and the GRK 2204. I.D. and B.M.S. acknowledge support by an ERA fellowship (01DT20010, BMBF). Open access funding enabled and organized by Projekt DEAL.

Conflict of Interest

The authors declare no conflict of interest.

Keywords: ionic liquids · nanoparticles · Rietveld refinement · titanium oxide · titanium oxyhydroxy fluoride

- [1] a) A. R. Dória, R. S. Silva, P. H. Oliveira Júnior, E. A. Dos Santos, S. Mattedi, P. Hammer, G. R. Salazar-Banda, K. I. B. Eguluz, *Electrochim. Acta* **2020**, *354*, 136625; b) K. Akiyoshi, T. Kameyama, T. Yamamoto, S. Kuwabata, T. Tatsuma, T. Torimoto, *RSC Adv.* **2020**, *10*, 28516–28522; c) M. Voggenreiter, P. Vöpel, B. Smarsly, S. Polarz, *Z. Anorg. Allg. Chem.* **2017**, *643*, 93–100.
- [2] B. Rodríguez-Cabo, E. Rodil, A. Soto, A. Arce, *J. Nanopart. Res.* **2012**, *14*, 1–10.
- [3] R. Luque, R. S. Varma, *Sustainable Preparation of Metal Nanoparticles*, Royal Society of Chemistry, Cambridge, **2012**.
- [4] P. Voepel, B. M. Smarsly, *Z. Anorg. Allg. Chem.* **2017**, *643*, 3–13.
- [5] a) T. Nakashima, N. Kimizuka, *J. Am. Chem. Soc.* **2003**, *125*, 6386–6387; b) S. Hu, H. Wang, J. Cao, J. Liu, B. Fang, M. Zheng, G. Ji, F. Zhang, Z. Yang, *Mater. Lett.* **2008**, *62*, 2954–2956; c) H. Choi, Y. J. Kim, R. S. Varma, D. D. Dionysiou, *Chem. Mater.* **2006**, *18*, 5377–5384; d) Y. Zhou, M. Antonietti, *J. Am. Chem. Soc.* **2003**, *125*, 14960–14961.
- [6] a) N. Yu, L. Gong, H. Song, Y. Liu, D. Yin, *J. Solid State Chem.* **2007**, *180*, 799–803; b) H. Kaper, F. Endres, I. Djerdj, M. Antonietti, B. M. Smarsly, J. Maier, Y.-S. Hu, *Small* **2007**, *3*, 1753–1763; c) S. S. Mali, C. A. Betty, P. N. Bhosale, R. S. Devan, Y.-R. Ma, S. S. Kolekar, P. S. Patil, *CrystEngComm* **2012**, *14*, 1920–1924.

- [7] a) H. Kaper, S. Sallard, I. Djerdj, M. Antonietti, B. M. Smarsly, *Chem. Mater.* **2010**, *22*, 3502–3510; b) V. Mansfeldova, B. Laskova, H. Krysova, M. Zukalova, L. Kavan, *Catal. Today* **2014**, *230*, 85–90.
- [8] T. P. Feist, P. K. Davies, *J. Solid State Chem.* **1992**, *101*, 275–295.
- [9] R. Marchand, L. Brohan, M. Tournoux, *Mater. Res. Bull.* **1980**, *15*, 1129–1133.
- [10] C. Wessel, L. Zhao, S. Urban, R. Ostermann, I. Djerdj, B. M. Smarsly, L. Chen, Y.-S. Hu, S. Sallard, *Chem. Eur. J.* **2011**, *17*, 775–779.
- [11] P. Voepel, C. Seitz, J. M. Waack, S. Zahn, T. Leichtweiß, A. Zaichenko, D. Mollenhauer, H. Amenitsch, M. Voggenreiter, S. Polarz, B. M. Smarsly, *Cryst. Growth Des.* **2017**, *17*, 5586–5601.
- [12] B. Li, Z. Gao, D. Wang, Q. Hao, Y. Wang, Y. Wang, K. Tang, *Nanoscale Res. Lett.* **2015**, *10*, 1–7.
- [13] P. Voepel, M. Sieland, J. Yue, I. Djerdj, B. M. Smarsly, *CrystEngComm* **2020**, *22*, 1568–1576.
- [14] W. Zheng, X. Liu, Z. Yan, L. Zhu, *ACS Nano* **2009**, *3*, 115–122.
- [15] D. Bahnemann, A. Henglein, L. Spanhel, *Faraday Discuss. Chem. Soc.* **1984**, *78*, 151.
- [16] L. S. Ott, M. L. Cline, M. Deetlefs, K. R. Seddon, R. G. Finke, *J. Am. Chem. Soc.* **2005**, *127*, 5758–5759.
- [17] J. Rodriguez-Carvajal, *FULLPROF - A program for Rietveld Refinement*, Laboratoire Leon Brillouin, CEA Saclay, France, **2000**.
- [18] J. Bijelić, A. Stanković, B. Matasović, B. Marković, M. Bijelić, Ž. Skoko, J. Popović, G. Štefanić, Z. Jagličić, S. Zellmer, T. Preller, G. Garnweitner, T. Đorđević, P. Cop, B. Smarsly, I. Djerdj, *CrystEngComm* **2019**, *21*, 218–227.
- [19] R. J. Hill, C. J. Howard, *J. Appl. Crystallogr.* **1987**, *20*, 467–474.
- [20] T. E. Weirich, M. Winterer, S. Seifried, H. Hahn, H. Fuess, *Ultramicroscopy* **2000**, *81*, 263–270.
- [21] R. Macchieraldo, L. Esser, R. Elfgen, P. Voepel, S. Zahn, B. M. Smarsly, B. Kirchner, *ACS Omega* **2018**, *3*(8), 8567–8582.

Manuscript received: September 4, 2020

Revised manuscript received: October 22, 2020

Correction added on 13.04.2022, after first online publication: Projekt DEAL funding statement has been added.